ELSEVIER

Diamond and Related Materials 10 (2001) 1968–1972

DIAMOND AND RELATED MATERIALS

www.elsevier.com/locate/diamond

Spectroscopic ellipsometry studies of nanocrystalline carbon thin films deposited by HFCVD

S. Gupta[a,1], B.R. Weiner[b], G. Morell[c,*]

[a] *Department of Physics, University of Puerto Rico, P.O. Box 23343, San Juan, PR 00931, USA*
[b] *Department of Chemistry, University of Puerto Rico, P.O. Box 23346, San Juan, PR 00931, USA*
[c] *Department of Physical Sciences, University of Puerto Rico, P.O. Box 23323, San Juan, PR 00931, USA*

Received 4 September 2000; accepted 24 January 2001

Abstract

Nanocrystalline carbon thin films were grown by hot-filament chemical vapor deposition (HFCVD) using a relatively high concentration of methane in hydrogen. The films were deposited on molybdenum substrates at 900°C, and under various substrate-biasing conditions. The optical properties were examined ex situ using spectroscopic phase-modulated ellipsometry (SPME) from the near IR to the near UV region (1.5–5.0 eV). The ellipsometry data [$\psi(\lambda_i)$, $\Delta(\lambda_i)$] were modeled using Bruggeman effective-medium approximation (EMA) and the dispersion relation for the amorphous semiconductor (Forouhi and Bloomer Model; Phys. Rev. B 34, 7018, 1986). We performed these simulations by least-square regression analysis (LRA) and obtained the true dielectric function of our nanocrystalline carbon material and the energy band-gap (E_g), along with the film thickness, bulk void fraction and roughness layer. We discuss the possible physical meaning of the five parameters in the amorphous dispersion model applied to the case of nanocrystalline carbon. Micro-Raman spectroscopy and profilometry were used to guide and validate the simulations.

Keywords: Nanocrystalline carbon; Electron- or ion-assisted deposition; Ellipsometry; Modeling; Chemical vapor deposition (CVD)

1. Introduction

A great deal of attention has been given to diamond and diamond-like carbon (DLC) thin films since their advent owing to a wide range of desired mechanical, optical and electronic properties (such as high mechanical hardness, chemical inertness, negative electron affinity and optical transparency) [2–4] that pave their way to several technological applications. It is well known that diamond-like carbon material has an extremely complex structure due to the different types of hybridization of carbon atoms: tetrahedral sp^3; trigonal sp^2; and linear sp^1. The addition of hydrogen atoms bonded to carbon causes the structure to be further complicated. Usually several properties of these nanocrystalline carbon (n-C) materials are attributed to the relative ratio and the spatial correlation of sp^3/sp^2 coordinated carbon [4], since the amount of sp^1 is negligible. For example, films having a high fraction of sp^3-coordinated C exhibit higher optical band-gap and hardness as compared to films rich in sp^2 C. A number of theoretical studies of various hypothetical phases of carbon have also been carried out, predicting such behavior [5].

A variety of optical characterization methods such as: reflectance and transmittance measurements [6]; Fourier transform infrared spectroscopy (FTIR) [7]; Raman spectroscopy [8]; spectroscopic ellipsometry (SE) [9–11]; and electron energy loss spectroscopy (EELS) [12] have been applied to the identification of

* Corresponding author. Tel.: +1-787-764-0000, ext. 2602; fax: 787-756-7717.
E-mail address: gmorell@rrpac.upr.clu.edu (G. Morell).
[1] National Science Foundation Graduate Fellow (NSF-EPS-9874782).

0925-9635/01/$ - see front matter
PII: S0925-9635(01)00387-9

the microstructure giving rise to the various optical and electronic properties. Typically, nanocrystalline and amorphous carbon films prepared by a variety of methods such as chemical vapor deposition (CVD), sputtering and pulsed laser evaporation (PLD) possess refractive index of 1.8–2.2, optical gap of 1–2 eV, and electrical resistivity of 10^4–10^8 Ω-cm [13,14].

In this study, we focus our attention on the spectroscopic ellipsometry optical characterization of nanocrystalline carbon thin films modified by low energy electron- and ion-bombardment. The optical constants of these materials are strongly dependent on the process deposition parameters, due to the corresponding structural variations. Particle bombardment during growth alters the film microstructure and, therefore, changes the electronic band structure of the material. This has interesting implications, since the low-energy particle bombardment creates a variety of defects in the material that can render it a viable cold-cathode for field emission applications.

We employed the dispersion model for amorphous materials proposed by Forouhi and Bloomer (FB) [1], which was derived on the basis of the extinction coefficient (k) for a single electron transition in the proximity of the interband energy gap (E_g):

$$k(E) = \frac{A(E - E_g)^2}{E^2 - BE + C} \tag{1}$$

Unlike Tauc's model, which is more commonly employed to evaluate the optical gap of amorphous semiconductors, the FB model does fulfill the causality principle [1], making it possible to arrive at the corresponding expression rigorously for the refractive index, $n(E)$, through Kramers–Kroning relations:

$$n(E) = n(\infty) + \frac{BE + C}{E^2 - BE + C} \tag{2}$$

A, B, C, $n(\infty)$ and E_g are fitting parameters, where E_g corresponds to the optical band-gap, $n(\infty)$ is the refractive index at optical frequencies, A is inversely proportional to the lifetime of the excited states, and B is related to the energy difference between the bonding and anti-bonding states [1]. C depends on both A and B.

This five-parameter model has been applied to the study of several disordered semiconductor materials [1]. According to the model, the optical absorption is dominated by a single type of electronic transition in the optical energy range involving states within ~5 eV of the Fermi level and hence should involve mostly π–π^* excitations. To investigate the optical absorption processes of the disordered carbon material in thin film form studied hereby, fits to the raw or pseudodielectric SE data were performed using Levenberg–Marquardt [15] algorithm, while varying all the parameters to fit simultaneously both the index of refraction and the extinction coefficient spectra. The results obtained for the films grown under particle bombardment are compared to those obtained for the film grown without substrate bias. Raman spectroscopy and profilometry were used to validate the results.

2. Experimental details

The nanocrystalline diamond thin films in this study were prepared in a custom-built hot filament chemical vapor deposition (HFCVD) reactor, described in detail by Morell et al. [16]. The three films were grown on mirror-polished molybdenum (Mo) disks of 1.4-cm diameter. All of the substrates were ultrasonically cleaned thoroughly in methanol for 15 min. They were then dried in He and placed immediately on a molybdenum substrate holder that is integrated with a graphite heater. The chamber was evacuated to 10^{-7} torr before introducing the clean reactive gas mixture.

Briefly, during the growth process a 10% CH_4/H_2 gas mixture, with a flow ratio of 20:80 and total flow of 100 sccm, was directed through a heated rhenium (Re) filament. The choice of Re for the filament material has the advantage that it does not react with carbon and therefore is not consumed during the diamond reaction. Re wire (8 cm) of 0.5-mm diameter was coiled, positioned 8 mm from the substrate, and Joule heated to 2400–2500°C as measured by an optical pyrometer (Dual-wavelength, Mikron M90 Model). The Mo substrate was mounted on a graphite heater to intercept the excited gas downstream from the filament. It was maintained at 950–1000°C during the growth process and the total gas pressure of the chamber was kept at 20 torr. Real-time in situ SE was used to calibrate the true temperature of the substrate surface. A polished commercial Si substrate was used for the calibration, and the E_1 transition energy from a line-shape analysis of the second derivative of the dielectric function provided the temperature of the surface, through the relationship $T[\mathrm{K}] = \{3.486 - E_1(\mathrm{eV})\}/4.07 \times 10^{-4}$ [16]. The resulting true temperature of the surface is typically ~50°C higher than that measured directly by a thermocouple embedded in the heater block.

In addition to the above mentioned conditions, a continuous positive (forward) or negative bias (reverse) were applied using a high-voltage power supply (BHK 1000-02). This bias voltage caused the substrate to be either bombarded with electrons or ions, for the positive and negative bias, respectively. Typical currents drawn for the low-energy electrons and ions were 200 mA (+343 V) and 50 mA (−323 V), respectively,

during the growth of the nanocrystalline carbon thin films. No intentional doping was employed and therefore the samples studied are intrinsic.

Typical film thickness were 0.6–2.5 μm for all the three samples, mechanically measured using a Tencor Alpha Step profilometer. The ex situ ellipsometry spectra were carried out with Jobin–Yvon UVISEL phase-modulated spectroscopic ellipsometer (Model DH10) in the NIR (1.5 eV) to near UV (5.0 eV) photon energy range with a fixed incident angle of 70° towards the sample. The actual film thickness deduced from ex situ ellipsometry was also compared with the mechanically measured one.

Atomic force microscopy (Digital Instrument, Nanoscope III) was used to investigate the surface morphology and roughness. The Raman spectra were recorded using an ISA Jobin–Yvon T64000 Raman spectrometer with approximately 1 cm^{-1} resolution. These spectra were excited with the 514.5-nm line of an Ar^+ laser kept at a laser power of 10 mW to avoid thermal effects on the measurements. The scattered light from a probed area of approximately 1–2 μm^2 was collected using an 80× objective.

3. Results and discussion

Shown in Fig. 1 are the Raman spectra for the three samples studied hereby depicting the typical broad features of disordered carbon material. A small narrow diamond signature (at 1332.5 cm^{-1}) is observed only for the no bias sample. Since the Raman cross-section of graphitic carbon is approximately 50 times larger than that of diamond [8], there must be a substantial amount of microcrystalline diamond inclusions in the film. Besides, a substantial amount of three-fold sp^2 coordinated/hybridized carbon is also present, indicated by the graphitic G-band at 1580 cm^{-1}. Generally speaking, the Raman band at 1360 cm^{-1} has contributions from both highly defective sp^3 carbon (diamond-like) and disordered sp^2 carbon (graphitic D-band [8]). A shoulder at 1150 cm^{-1} is observed in the spectra of the no bias and reverse bias samples indicating the presence of nanocrystalline diamond phases (also sp^3 C) in the films [17].

Ex situ SE was employed to investigate the optical properties of the three films. The experimental ex situ SE spectra and the corresponding FB dispersion fits for psi [$\psi(\lambda_i)$] and delta [$\Delta(\lambda_i)$] using the Levenberg–Marquardt regression algorithm are shown in Fig. 2. The results were fitted employing Bruggeman Effective Medium Theory (BEMT) [18] under the assumption that the film composition is an aggregate mixture of disordered sp^3 and sp^2 carbon (sp^3 C, sp^2 C). A two-layer microstructural model, shown in Fig. 3, was the simplest model found to simulate the data reasonably well. This model consists of a surface roughness layer (defined as 50% voids and 50% FB-modeled material), followed by a dense amorphized FB-modeled material layer. The Mo substrate is last, assumed to be infinite since the light does not bounce back after passing through it.

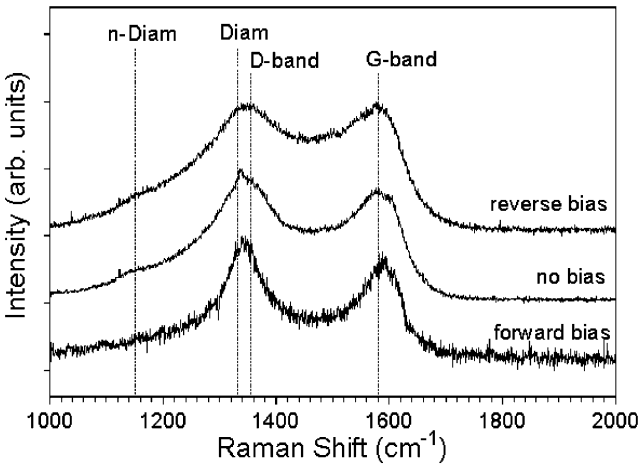

Fig. 1. Raman spectra of the nanocrystalline carbon (n-C) thin films deposited by hot-filament CVD depicting the typical signatures of diamond and disordered carbon material.

The degree of agreement between the model and the

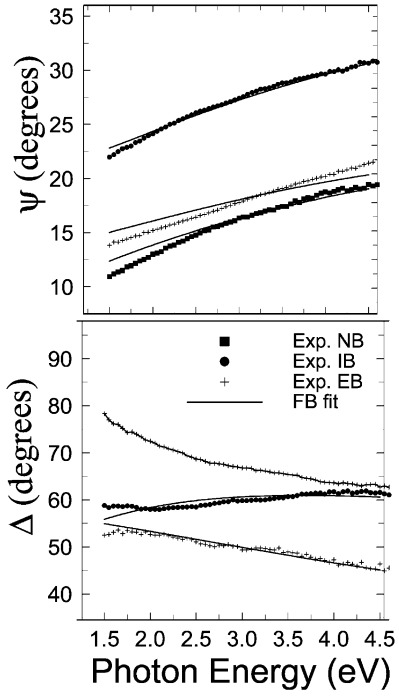

Fig. 2. The raw SE data (experimental) and the FB fit (simulated) for the psi (degrees) and delta (degrees) are shown as a function of photon energy for nanocrystalline carbon (n-C) thin films deposited by hot-filament CVD under different substrate biasing conditions. The Experimental data for the no bias, electron bombardment and ion bombardment films is denoted as Exp. NB, EB and IB, respectively, in the graph.

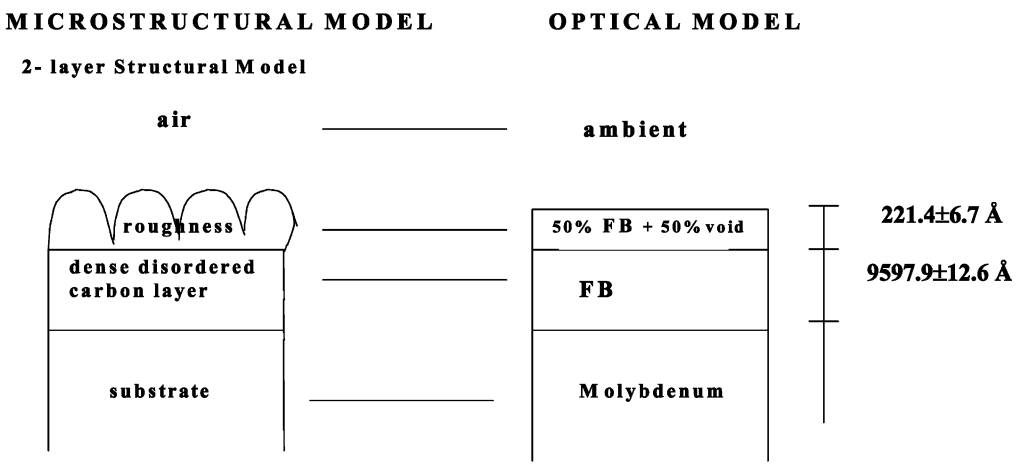

Fig. 3. The microstructural model and the corresponding optical model to describe nanocrystalline carbon (n-C) in least-squares linear regression analysis fits to the ellipsometry data shown in Fig. 2.

ellipsometry data can be evaluated from Fig. 2. Qualitatively, these are the best fits, while quantitative results are provided in Table 1. The overall thicknesses of the films derived from the SE model are pretty much in agreement with those measured mechanically (not shown) using a profilometer. Results in terms of the bonding–antibonding state energy difference ($E_\pi - E_\pi^*$), which is a sort of average Penn gap and excited state lifetime obtained from the B and A values, respectively, are listed in Table 1. The findings of the optical gap ~ 1.2–2.2 eV are in agreement with the fact that the films contain a relatively high fraction of sp^2 bonded carbon. The order of the energy band-gap and the refractive index at optical frequency for the three films studied hereby are as follows: $(E_g)_{NB} > (E_g)_{IB} > (E_g)_{EB}$ and $n(\infty)_{NB} < n(\infty)_{IB} < n(\infty)_{EB}$. There appears to be an inverse relation between the value of $n(\infty)$ and the band-gap (E_g), in agreement with the observations made for sputtered a-C and a-C:H films studied with the same model [19].

In the photon energy range studied hereby of 1.5–5.0 eV, the π–π^* transitions (sp^2 clusters) are the predominant absorption processes involved, while the interband σ–σ^* electronic transitions resulting from sp^3 C bonding lie in the UV energy range (≥ 5.5 eV). As observed from the Raman signatures (Fig. 1), there are micro/nanocrystalline diamond inclusions in the film prepared with no bias and, correspondingly, its band-gap is higher and the excited state lifetimes longer (smaller A) than those of the films grown with low-energy particle bombardment. These values then change as a result of particle bombardment, which enhances the formation of mid-gap states within the band structure of the material through the formation of sp^2 C bonds, resulting in lower band-gaps and shorter excited state lifetimes (larger A).

4. Conclusions

Nanocrystalline carbon thin films were grown by hot-filament chemical vapor deposition (HFCVD) using a relatively high concentration of methane in hydrogen. The optical properties of these films were investigated using ex situ spectroscopic ellipsometry. Analysis of the SE data using the well-known Forouhi and Bloomer model provided information about the electronic structure of these nanocrystalline carbon thin films. Non-diamond carbon introduces π–π^* transitions within the diamond band-gap that reduce the effective band-

Table 1
EMA simulation results for nanocrystalline carbon thin films grown by HFCVD under various substrate biasing conditions[a]

Sample							
Growth parameters	Thickness (Å)	A	B (eV)	C (eV^2)	n (∞)	E_g (eV)	χ^2 (best-fit)
900°C no bias	9819.3 ± 19.7	0.190	4.108	13.916	1.714	2.701	0.16
900°C forward bias (+343 V, 200 mA)	4423.7 ± 21.5	0.829	1.63	4.586	2.257	1.170	0.66
900°C reverse bias (−323 V, 50 mA)	21844.4 ± 172.4	0.795	1.991	7.212	2.055	1.672	1.11

[a] Other deposition parameters are: $[CH_4] = 2.0\%$ in high hydrogen dilution; pressure = 20.0 torr; and number of deposition hours = 6 h for all of the samples.

gap of the composite material. Low energy particle bombardment (either with electrons or ions) of the growing film was found to reduce the micro/nanocrystalline diamond components. This reduction in the amount of ordered sp^3 carbon was accompanied by a reduction of the effective band-gap and of the excited state lifetimes. Consequently, the influence of low-energy particle bombardment (both electron and ion) is to increase the sp^2 C content through defect states within the electronic band-gap (mid-gap or localized states) which decreases the optical gap and shortens the lifetime of the excited states.

Acknowledgements

This research work is supported by the Department of Defense (DoD ONR Grant No. N00014-98-1-0570), the Department of Energy (DoE Grant No. DE-FG02-99ER45796) and the University of Puerto Rico (UPR FIPI Grant No. 880344).

References

[1] A.R. Forouhi, I. Bloomer, Phys. Rev. B 34 (1986) 7018.
[2] J.C. Angus, P. Koidl, S. Domitz, in: J. Mort, F. Jansen (Eds.), Plasma Deposited Thin Films, CRC Press, Boca Raton, FL, 1986, p. 89.
[3] M.N. Yoder, in: K.E. Spear, J.P. Dismukes (Eds.), Synthetic Diamond: Emerging CVD Science and Technology, John Wiley and Sons, New York, 1994, p. 4.
[4] J. Robertson, Adv. Phys. 35 (1986) 317.
[5] D.R. Mckenzie, D.A. Muller, B.A. Paithorpe, Phys. Rev. Lett. 67 (1991) 773.
[6] N. Savvides, E-MRS Meeting 17 (1985) 275.
[7] B. Dischler, A. Bubenzer, P. Koidl, Solid State Commun. 48 (1983) 105.
[8] R.J. Nemanich, J.T. Glass, G. Luckovsky, R.E. Shroder, J. Vac. Sci. Technol. A 6 (1988) 1783 (and references therein).
[9] E. Pascual, C. Serra, E. Bertran, Surf. Coat. Technol. 47 (1991) 263.
[10] D.E. Aspnes, A.A. Studna, Phys. Rev. B 27 (1983) 985.
[11] B. Hong, J. Lee, R.W. Collins et al., Diam. Relat. Mater. 6 (1997) 55.
[12] P.J. Fallon, V.S. Veeraswamy, C.A. Davis et al., Phys. Rev. B 48 (1993) 4777.
[13] M. Yoshikawa, Mater. Sci. Forum 52 and 53 (1989) 365.
[14] J. Robertson, Mater. Res. Soc. Symp. Proc. 509 (1998) 83–88.
[15] D.W. Marquardt, J. Soc. Indis. Appl. Math. 11 (1963) 431.
[16] G. Morell, E. Canales, B.R. Weiner, Diam. Relat. Mater. 8 (1999) 160.
[17] H. Eto, Y. Tamou, Y. Oshawa, N. Kikuchi, Diam. Relat. Mater. 1 (1992) 372.
[18] D.A.G. Bruggeman, Ann. Phys., Leipzig 24 (1935) 636.
[19] W.A. McGahan, J.A. Wollam, Proc. Mater. Res. Soc. Symp. 349 (1994).